International Journal of Industrial Ergonomics 44 (2014) 561–569

Contents lists available at ScienceDirect

International Journal of Industrial Ergonomics

journal homepage: www.elsevier.com/locate/ergon

Effects of body-borne equipment on occupant forces during a simulated helicopter crash

Daniel Aggromito [a,b], Bernard Chen [a], Rodney Thomson [b,c], John Wang [d], Wenyi Yan [a,*]

[a] Department of Mechanical & Aerospace Engineering, Monash University, Clayton, Victoria 3800, Australia
[b] Cooperative Research Centre for Advanced Composite Structures, 1/320 Lorimer Street, Port Melbourne, Victoria 3207, Australia
[c] Advanced Composite Structures Australia Pty Ltd, 1/320 Lorimer Street, Port Melbourne, Victoria 3207, Australia
[d] Defence Science and Technology Organisation, 506 Lorimer Street, Fishermans Bend, Victoria 3207, Australia

A R T I C L E I N F O

Article history:
Received 30 October 2013
Received in revised form
28 February 2014
Accepted 10 March 2014
Available online

Keywords:
Dimensional analysis
Biodynamics
Crashworthy seat
Helicopter
Occupant loads

A B S T R A C T

Helicopter seats are designed to a specified mass range including equipment and can only provide limited energy absorbing protection within its designed energy absorbing capability. Over recent years, military occupants have been required to carry increasing amounts of equipment, which may affect the probability of injury during a crash. To investigate the effects of increasing equipment mass during a helicopter crash on injury, a linear 7-degree-of-freedom mass–spring–damper model is developed to simulate an occupant wearing body-borne equipment on a crashworthy helicopter seat. A fixed load energy absorption mechanism is also included in the model. To examine the effects of equipment attachment types, the mass bodies representing the equipment are attached with a spring and damper, with low and high stiffness values indicating loose and tight attachment respectively. Dimensional analysis shows that the maximum forces are proportional to the initial impact velocity prior to stroke. The results demonstrate that increasing the equipment mass reduces the seat's capability to absorb the total impact energy at higher initial impact velocities. The safe velocity, the velocity that prevents bottoming out, reduces from 10.2 m/s, for an occupant without equipment, to 7.4 m/s for an occupant with an equipment mass of 40 kg at the lower and upper torso and 2 kg at the head. When the equipment mass is 40 kg at the hip and at the upper torso and 2 kg at the head, a maximum increase on the underside of the pelvis of 173% is measured, providing an increased possibility of injury in the lumbar region. Increases of 321%, 889% and 335% on the maximum forces on the hip, upper torso and head respectively create the potential for contact injury at the hip, upper torso and head from equipment and more than a 50% chance of spinal injury. The results show that increasing equipment mass significantly increases the potential for injury at the lumbar, hip, upper torso and head.

Relevance to industry: Relevance to industry: Military pilots today are required to wear a vast amount of equipment, that exceeds the weight limit of crashworthy helicopter seats. This paper demonstrates the disastrous effects of wearing large amounts whilst seated on a crashworthy helicopter seat in a simulated helicopter crash.

1. Introduction

In a helicopter crash, a crashworthy seat is designed to absorb the energy through a stroking load limit mechanism. This mechanism allows the seat and the occupant to move at loads just under the humanly tolerable limit, over the maximum distance between the seat pan and the cabin floor (Coltman, 1994). The seat is designed in terms of a specified range of occupant mass and can only provide limited protection within its designed energy absorbing capability (Desjardins, 2003). Military Standard-58095A (1986) is the standard used for aircrew seat design. It sets the condition that a crashworthy seat must be designed to carry an occupant with 5 kg of equipment during a crash. Current body-borne equipment can exceed six times that depending on mission type (NAVAIR 13-1-6.7.2, 1999). If the increased mass causes the impact energy to be excessive, a phenomenon called bottoming out will occur at the end of stroke. Bottoming out occurs, because the stroke is initiated at lower acceleration and causes the seat to reach its full stroking distance before the total

Abbreviations: DOF, degrees of freedom; ATD, anthropomorphic test device; EQM, equations of motion.

* Corresponding author. Tel.: +61 (3) 9902 0113.
E-mail address: Wenyi.Yan@monash.edu (W. Yan).

http://dx.doi.org/10.1016/j.ergon.2014.03.002
0169-8141/© 2014 Elsevier B.V. All rights reserved.

impact energy is absorbed resulting in the occupant potentially experiencing a significantly higher impact load and increasing the likelihood of injury. The effect of weight on bottoming out occurring and the subsequent extreme loads experienced by an occupant are illustrated in a crash of a Sikorsky S-92A helicopter, where 17 passengers died of drowning. It was found that four seats bottomed out due to the weight of the individuals. All occupants on seats excluding those that bottomed out experienced inertial vertical load factors of between 5.3 g and 8.6 g, however, the individuals on seats that bottomed out experienced inertial vertical load factors that most likely exceeded 8.6 g (Transport Safety Board of Canada, 2009).

Lumped parameter models consider the human body as several concentrated masses connected by a spring and damper and are the simplest method to represent the human body (Liang and Chiang, 2006). A four-degree of freedom (DOF) model developed by Payne and Band (1971) was used in vertical vibrations for seated occupants and based on the one-DOF system developed earlier by Payne and Stech (1969), which used one mass body to represent the human body. Adding to that model, they added the viscera, the buttocks and a head to more accurately represent the specific mass bodies of the human body. The parameters of the model were selected by matching relevant available data from vertical drop tests and calculating the driving point impedance characteristics. Similarly, Wan and Schimmels (1995) developed a four-DOF model with the same mass bodies, however the viscera is attached to both the upper torso and lower torso. This model was considered in a literature review by Liang and Chiang (2006) to provide the greatest accuracy with experimental values in Boileau and Rakheja (1998) in seat to head transmissibility, driving point impedance and the apparent mass.

A number of studies have been completed on seated occupants in landmine blasts, underwater shock and injury from aviation helmet neck loading (Wang and Bird, 2000; Zong and Lam, 2002; Dong and Lu, 2012; Mathys and Ferguson, 2012). However, research is limited on the effects of body-borne equipment on injury in a helicopter crash. Richards and Sieveka (2011) developed a model using the software MADYMO to investigate lumbar loads with increasing equipment mass. The occupant was modelled as an ellipsoid Hybrid III Anthropomorphic Test Device (ATD) with a rigid mass on the upper torso to represent equipment. The addition of 30 lb of equipment mass resulted in a predicted 61% increase in lumbar load. Only the influence of rigid upper torso equipment mass on lumbar load was considered. Furthermore, the effect of equipment attachment types on loading and loading paths was not considered in Richards and Sieveka (2011).

To be able to fully analyse the effect of body-borne equipment on the forces on an occupant, equipment needs to be located at the hip, upper torso and head and attachment types need to be examined to investigate the influence on the loads.

The objective of this study is to determine the forces as a result of increasing the equipment mass on an occupant seated on a crashworthy seat during a helicopter crash. A four-DOF occupant model is used to represent a seated occupant. Equations were devised to represent the force control of a crashworthy seat utilising a fixed load energy absorption (FLEA) device. Equipment was attached at the hip, upper torso and head with a spring and damper, and the spring coefficient was varied to examine the effects of loose and tight attachment types on the forces and loading paths on the occupant. Using a simple numerical procedure with a transient analysis, the model was solved by the Fourth-Order Runge–Kutta method in MATLAB used in the ODE45 function.

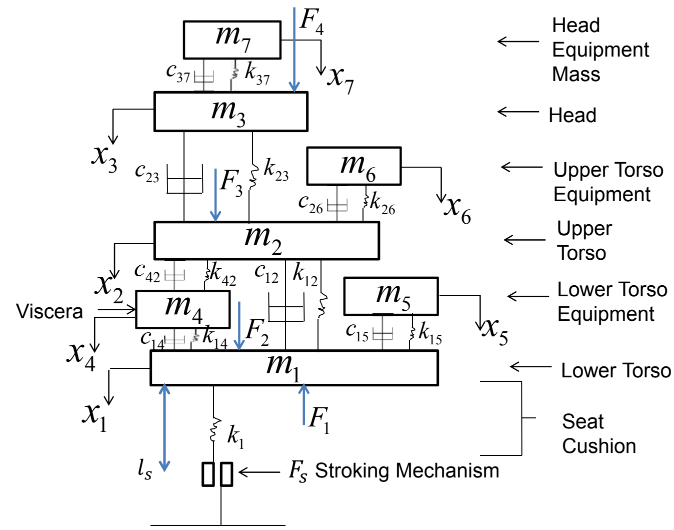

Fig. 1. Occupant model with equipment attached.

2. Biodynamic occupant model with equipment

2.1. Occupant model

The occupant model is a four-DOF mass–spring–damper model that closely replicates that proposed by Payne and Band (1971) and Wan and Schimmels (1995), see Fig. 1. The occupant is represented by 4 mass bodies, the lower torso (m_1), upper torso (m_2), head (m_3) and viscera (m_4). The spring coefficient is represented by k and the damping coefficient by c. The subscript values following the spring and damping coefficients are used to represent the masses it connects. For example, k_{12} joins m_1 with m_2. The viscera is identified as one of the most important subsystems, when excited in the sitting position as under the influence of longitudinal vibration the abdominal mass vibrates in and out of the thoracic cage. A spring and damper characterizes the spinal column and connects the upper torso to the lower torso. To accurately calculate spinal response and the force from the helmet on the head, the upper torso and the head are considered as two mass bodies also connected by a spring and a damper. The pelvis and the seat are identified as one mass body and is the major difference from the model in Wan and Schimmels (1995), with the seat cushion represented as a spring with non-linear characteristics. The mass, stiffness and damping properties were determined from the models proposed by Payne and Band (1971) and Wan and Schimmels (1995). The occupant has an effective mass of 62.5 kg which is based on a 50th percentile male occupant. The model parameters are presented in Table 1.

Table 1
Occupant parameters.

Item	Location	Value
m_1 (kg)	Lower torso	35
m_2 (kg)	Upper torso	17.5
m_3 (kg)	Head	4.5
m_4 (kg)	Viscera	5.5
k_{12} (kN/m)	Lower torso–Upper torso	150
k_{14} (kN/m)	Lower torso–Viscera	2
k_{23} (kN/m)	Upper torso–Head and neck	160
k_{42} (kN/m)	Viscera–Upper torso	12.5
c_{12} (kN s/m)	Lower torso–Upper torso	0.81
c_{14} (kN s/m)	Lower torso–Viscera	0.05
c_{23} (kN s/m)	Upper torso–Head and neck	0.424
c_{42} (kN s/m)	Viscera–Upper torso	0.131

Table 2
Helmet parameters.

Attachment type	Area (m^2)	Length (m)	Spring coefficient (kN/m)
Loose	0.0019	0.31	3.97
Semi-tight	0.066	0.34	6.03
Tight	0.145	0.38	10

2.2. Equipment mass investigated and attachment type

The equipment is modelled at the hip, the upper torso and the head to mimic real life mission operations. A typical occupant wears equipment at a number of locations as illustrated in Fig. 2(a). The equipment is distributed over the occupant at the lower torso and upper torso. This figure does not show the head mass. Fig. 2(b) illustrates the equipment and displays a key to indicate where the equipment worn by the occupant is located. The equipment mass varies from 10 kg to a maximum of 40 kg at the hip and upper torso, and the head equipment mass from 0.5 kg to 2 kg. The equipment masses investigated are based on the equipment list compiled in Richards and Sieveka (2011) for a U.S. Navy rotorcraft aviator. This list of equipment can range from 5 kg to over 30 kg when wearing full biological and chemical gear. The range of head equipment mass modelled helmets with and without night vision goggles and counterweight balances (Forde et al., 2011). The equipment mass at the lower torso is represented by m_5, at the upper torso by m_6 and the head by m_7 and is attached to the occupant with a spring and damper at each location. As with the designations of the symbols for the occupant, the spring and damping coefficients for the equipment attachments are represented by k and c respectively, with the subscript numbers following the symbols indicating the two bodies that the spring and damper connect. The attachment types vary from loose attachment to tight attachment, to consider the diverse equipment types that range from body armour with tight attachments to hand guns with loose attachments. A loose attachment at the lower torso (k_{15}) and upper torso (k_{26}) is simulated by a low stiffness coefficient (30 kN/m), semi-tight equipment attachment by a medium stiffness coefficient (60 kN/m) and tight equipment attachment by a high stiffness coefficient (90 kN/m). The values are chosen as an arbitrary guide to simulate the diverse attachment types, but do not aim to represent cases with slack in the attachment. It is believed that a lower stiffness coefficient will provide higher loading in alternate directions to the vertical direction and therefore a lower loading in the vertical direction, whereas a higher stiffness coefficient will provide a greater loading in the vertical direction and a smaller loading in the alternate directions. A stiffness coefficient in the middle of the range, that is a semi-tight attachment, will cause a load in the vertical plane in between the loadings generated by the tight attachment and loose attachment. The vertical direction, however, was the only direction analysed in this study.

The stiffness coefficient used for the head equipment attachment, which represents the foam helmet liner, was estimated by

$$k = \frac{EA}{L} \tag{1}$$

where E is the Young's modulus; A is the cross-sectional area of liner and L is the length.

This equation utilises the elastic modulus to calculate the axial stiffness of an element in tension or compression (Rao, 2005). A Young's modulus of 625 kPa for replica foam of the helmet liner was determined by measuring the elastic section of the stress–strain graph (Mills, 2007). For a loose and tight attachment, the thickness and length of the liner were assumed to be the lowest and highest value available and based on the liner of the HGU-84/P helmet (Mills, 2007). The values for the head equipment attachment are in Table 2.

The damping coefficients for all equipment attachments were estimated by

$$\zeta = \frac{c}{\sqrt{mk}} \tag{2}$$

where ζ is the damping ratio; m is the mass of the body and k is the stiffness coefficient.

A sensitivity analysis conducted by the authors was used to determine the effects of the damping ratio. An underdamped condition of 0.1 and 0.5 and a critically damped condition of 1 were the damping ratios investigated. It was found that the effect on the maximum force was negligible with the two underdamped conditions producing maximum forces within 0.2% and the critically damped condition a difference of 3%. Consequently an underdamped condition of 0.5 was used. Furthermore, in real-world operations, it would be assumed that there would be some oscillations of the attachment before returning to zero.

2.3. Equations of motion

For the model, the equations of motion of the masses are governed by a set of differential equations that can be written in the general matrix form

$$\boldsymbol{M}\ddot{X} + \boldsymbol{C}\dot{X} + \boldsymbol{K}X = \boldsymbol{F} \tag{3}$$

where $\boldsymbol{M}$, $\boldsymbol{C}$ and $\boldsymbol{K}$ are the mass, the damping coefficient and the stiffness coefficient matrices respectively

$$\boldsymbol{M} = \begin{bmatrix} m_1 & 0 & 0 & 0 & 0 & 0 & 0 \\ 0 & m_2 & 0 & 0 & 0 & 0 & 0 \\ 0 & 0 & m_3 & 0 & 0 & 0 & 0 \\ 0 & 0 & 0 & m_4 & 0 & 0 & 0 \\ 0 & 0 & 0 & 0 & m_5 & 0 & 0 \\ 0 & 0 & 0 & 0 & 0 & m_6 & 0 \\ 0 & 0 & 0 & 0 & 0 & 0 & m_7 \end{bmatrix}$$

$$\boldsymbol{C} = \begin{bmatrix} c_{14}+c_{12}+c_{12} & -c_{12} & 0 & -c_{14} & -c_{15} & 0 & 0 \\ -c_{12} & c_{42}+c_{12}+c_{23}+c_{26} & -c_{23} & -c_{42} & 0 & -c_{26} & 0 \\ 0 & -c_{23} & c_{23}-c_{37} & 0 & 0 & 0 & c_{37} \\ -c_{14} & -c_{42} & 0 & c_{14}+c_{42} & 0 & 0 & 0 \\ -c_{15} & 0 & 0 & 0 & c_{15} & 0 & 0 \\ 0 & -c_{26} & 0 & 0 & 0 & c_{26} & 0 \\ 0 & 0 & -c_{37} & 0 & 0 & 0 & c_{37} \end{bmatrix}$$

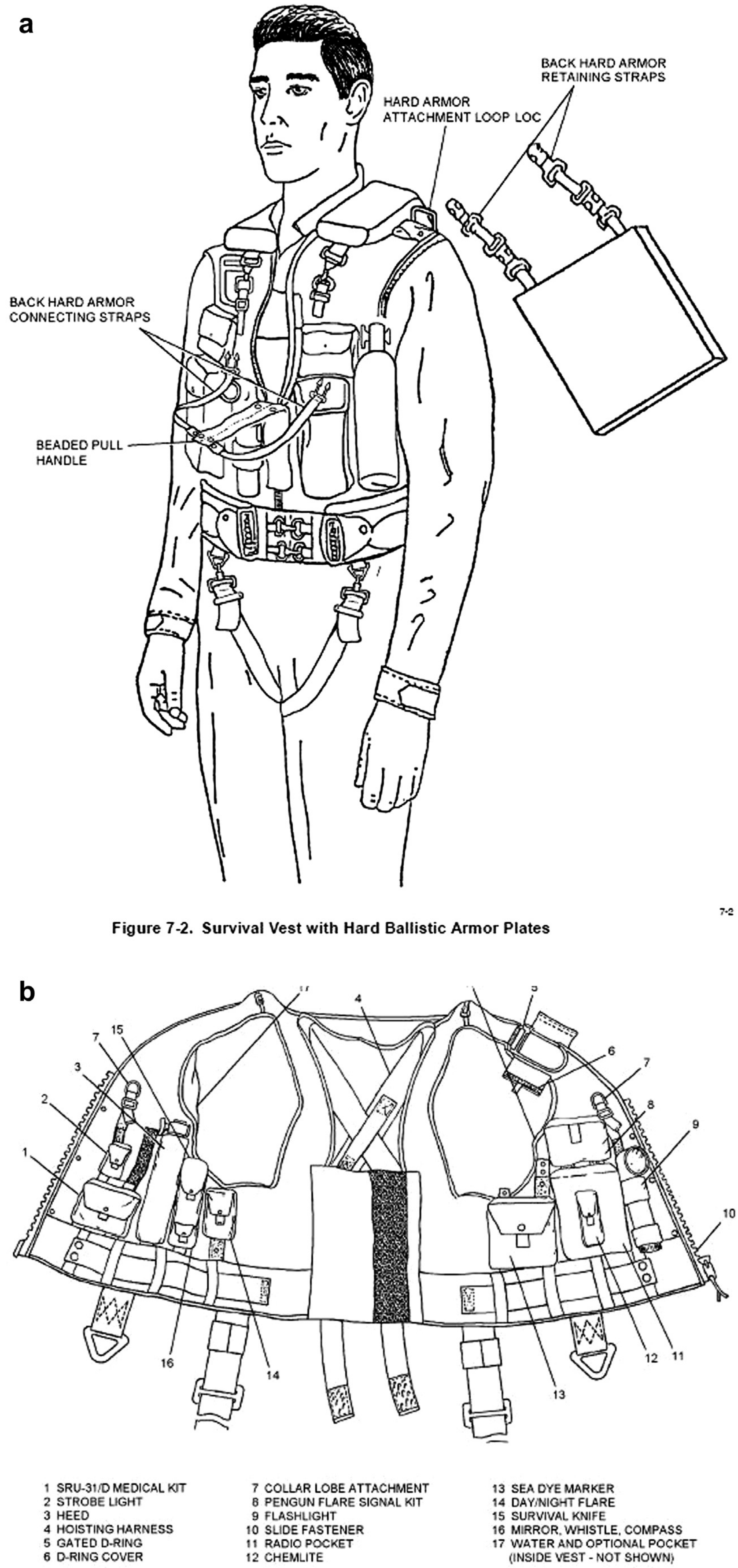

Fig. 2. (a) A typical aircrew ensemble on occupant and (b) the ensemble with more detail of equipment (Naval Air Systems Command, 1999).

and

$$\boldsymbol{K} = \begin{bmatrix} k_{14}+k_{12}+k_{15} & -k_{12} & 0 & -k_{14} & -k_{15} & 0 & 0 \\ -k_{12} & k_{42}+k_{12}+k_{23}+K_{26} & -k_{23} & -k_{42} & 0 & -k_{26} & 0 \\ 0 & -k_{23} & k_{23}-k_{37} & 0 & 0 & 0 & k_{37} \\ -k_{14} & -k_{42} & 0 & k_{14}+k_{42} & 0 & 0 & 0 \\ -k_{15} & 0 & 0 & 0 & k_{15} & 0 & 0 \\ 0 & -k_{26} & 0 & 0 & 0 & k_{26} & 0 \\ 0 & 0 & -k_{37} & 0 & 0 & 0 & k_{37} \end{bmatrix}$$

$$\boldsymbol{F} = \begin{bmatrix} F_1 \\ 0 \\ 0 \\ 0 \\ 0 \\ 0 \\ 0 \end{bmatrix} \tag{4}$$

$\boldsymbol{X} = [x_1 \quad x_2 \quad x_3 \quad x_4 \quad x_5 \quad x_6 \quad x_7]^{\mathrm{T}}$ is a column vector containing the displacement of the 7 masses from Fig. 1 from their equilibrium positions. These displacements are functions of time t and represent the freedom of the model. $\dot{\boldsymbol{X}}$ and $\ddot{\boldsymbol{X}}$ are vectors containing the velocities and accelerations.

The term F_1 represents the energy absorption of a crashworthy seat and depending on the stage of stroke, determines which part of equation (5) is inputted into the $\boldsymbol{F}$ matrix.

2.4. Equations to represent a crashworthy seat

Conceptually, the dynamic load on a seat stroke mechanism equals the product of the mass of occupant (including the equipment carried) and its acceleration. An FLEA device applies a single, fixed, approximately constant load to decelerate the occupant over a defined displacement, known as stroke (Desjardins, 2003).

Force 1 in Fig. 1 represents the force imparted on the occupant from the crashworthy seat. It is modelled with three equations to accurately replicate a crashworthy seat over the stages of the energy absorption in a crash impact, ‘before stroke’, ‘during stroke’ and if the load is excessive, bottoming out.

In this study, the stroke limit force decelerates only the effective occupant mass. The limit load is the standard limit load designed for a 50th percentile male occupant at 13,046 N (Desjardins, 2003). The force control during the energy absorption stage of a crashworthy seat is represented by

$$\begin{array}{lll} F_1 = k_1 x_1 & x_1 < l_{\mathrm{i}} & \text{Before Stroke} \\ F_1 = F_{\mathrm{s}} = 13,046N & l_{\mathrm{i}} < x_1 < l_{\mathrm{s}} & \text{During Stroke} \\ F_1 = 4k_1(x_1 - l_{\mathrm{s}}) & x_1 > l_{\mathrm{s}} & \text{Bottoming out} \end{array} \tag{5}$$

where x_1 is the displacement of the seat and hip, l_{i} is the initial displacement determined for the seat to reach its limit load and l_{s} is the maximum stroking length where the stroking stop is set. l_{i} is 217 mm and is calculated by dividing the stroking load F_{s} by the spring coefficient k_1. The stroking stop is set at 370 mm and is the average stroking length from two drop tests of a UH-60 crew seat (Richards and Sieveka, 2011).

The force/displacement curve for the crashworthy seat is illustrated in Fig. 3. Before stroke, on impact, the limit load is reached at l_{i}. During stroke, the force of the crashworthy seat is equal to the stroking load until the occupant’s velocity comes to zero or the seat stroke passes the stroking stops where bottoming out occurs. During bottoming out the spring coefficient of the seat is multiplied by 4.

To solve the EQM a time domain analysis is used, which concerns the real-time results of the simulation. To achieve real-time results, the fourth-order Runge–Kutta method employed by the ODE45 function in MATLAB is used. This method reduces second order differential equations to first order differential equations.

2.5. Model validation

To verify the model was producing reasonable results, the model inputs were adjusted to be identical to the 50th percentile ellipsoid hybrid III ATD with 18 kg equipment mass modelled in MADYMO on an FLEA seat in Richards and Sieveka (2011). In this study, an initial deceleration impulse on the cabin floor and an initial velocity of 10.2 m/s for the seat and occupant was modelled. In the comparison conducted here, an identical initial velocity was simulated, but not the deceleration impulse at the cabin floor. The results predicted a maximum lumbar load of 14.5 kN which correlated within 20% of the predicted lumbar load in that study.

3. Results

3.1. The effect of initial velocity

Dimensional analysis is a powerful tool to systematically examine a research problem and it has been successfully applied to study a biomechanics problem, e.g., a recent study on the resonant frequency of rat whiskers by Yan et al. (2013). Here, a dimensional analysis was carried out to understand the functional relationship between the output force and the initial impact velocity before bottoming out occurs. Any maximum force measured before stroke, represented by $F_{\max}$, acting on any mass in the model during such an impact process (such as the maximum force on the underside of

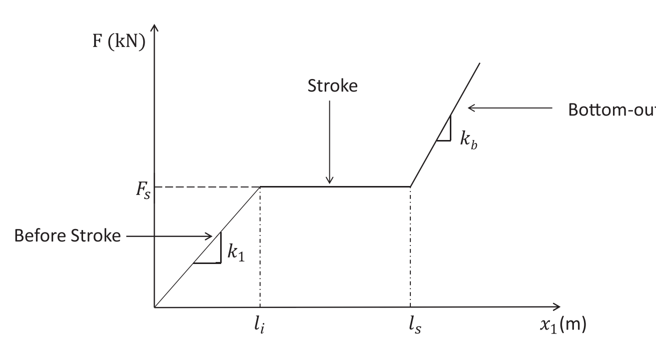

Fig. 3. Stroking load profile for the crashworthy seat.

the pelvis or the maximum force on the hip discussed in following subsections) depends on all the stiffness coefficients k_i, all the damping coefficients c_i, mass m_i ($i = 1, \ldots, 7$) and the initial velocity v_0:

$$F_{\max} = f(k_1, k_2, k_3, k_4, k_5, k_6, k_7, c_1, c_2, c_3, c_4, c_5, c_6, c_7, m_1, m_2, m_3, m_4, m_5, m_6, m_7, v_0) \tag{6a}$$

The Buckingham Π theorem for dimensional analysis states that the number of parameters can be reduced by using dimensionless parameters (Buckingham, 1914). For this case, mass m_1, stiffness coefficient k_1 and initial impact velocity v_0 are chosen as the primary quantities that represent the fundamental dimensions of the problem (kg, m, s). The force equation can be represented by the dimensionless function Π as

$$F = v_0\sqrt{m_1k_1}\prod\left(\frac{k_2}{k_1}, \ldots, \frac{k_7}{k_1}, \frac{c_2}{\sqrt{m_1k_1}}, \ldots, \frac{c_7}{\sqrt{m_1k_1}}, \frac{m_2}{m_1}, \ldots, \frac{m_7}{m_1}\right) \tag{6b}$$

Eq. (6b) clearly shows that the normalised maximum force on any part of the occupant is proportional to the initial impact velocity and such a linear relationship has been confirmed by numerical results. It is worth noting that this conclusion from the simple dimensional analysis is actually independent on how the problem is simulated because the equations of motion as formulated in Eq. (4) were not used in the dimensional analysis to derive Eq. (6b).

3.2. Effect of equipment on initial impact velocity to cause bottoming out

The effect of equipment mass on the minimum initial impact velocity to cause bottoming out is an important parameter to determine an allowable initial impact velocity for each equipment mass condition. This allowable initial impact velocity is the safe velocity preventing bottoming out from occurring.

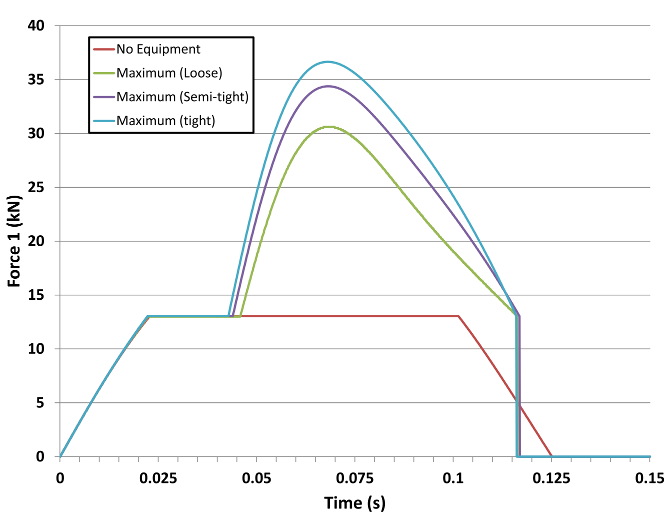

Fig. 4. Variation of the force control of the crashworthy seat (force 1) of an occupant wearing the maximum equipment mass with different equipment attachments compared to the case with no equipment as displacement increases.

The seat force is displayed in Fig. 3 for the occupant without equipment and the occupant with the maximum equipment mass and different attachment types. In this figure, the occupant without equipment does not surpass the limit load and the impact energy is absorbed prior to the seat reaching its full stroking distance, preventing bottoming out. The initial impact velocity used to retrieve this result is 10.2 m/s in the vertical (y) plane and is the safe initial impact velocity for the nude occupant. Therefore, the results in the following subsections are measured from a simulation with an initial impact velocity of 10.2 m/s as this is the safe velocity for the occupant without equipment. As equipment mass is added, the seat is no longer able to absorb all the impact energy prior to stroke finishing and, therefore, bottoming out occurs as illustrated in Fig. 4. Consequently, 10.2 m/s is not a safe impact velocity for the occupant with any equipment mass.

Table 3 indicates the minimum initial impact velocity at different equipment masses and attachment types to cause bottoming out. The initial impact velocity was varied by 0.1 m/s from 7 m/s to 10.2 m/s and the simulation was conducted to determine the minimum initial impact velocity to cause bottoming out for each equipment mass condition. Any initial impact velocity below these velocities in Table 3 for each condition indicates a safe velocity and the seat will be able to absorb the total impact energy regardless of the equipment mass. As the equipment mass increases and the attachments become tighter, the initial impact velocity to cause bottoming out reduces. Without equipment mass, the seat is able to withstand a higher impact velocity of 10.2 m/s, whereas with maximum equipment mass, tightly attached, the seat is only able to withstand an initial impact velocity of 7.4 m/s. Therefore, the initial impact velocity the seat is able to withstand reduces by 2.8 m/s. This demonstrates that the adverse effect equipment mass has on the seats ability to absorb the total impact energy at higher initial impact velocities.

3.3. Force on the underside of the pelvis

In this study, the force 1 is the force provided by the seat on the pelvis. As the seat and the pelvis are the same mass body, this force is imparted on the lumbar region and allows the prediction of injury in that area. When the occupant is not wearing equipment, the load is controlled at 13,046 N and bottoming out does not occur. When the occupant is wearing equipment, bottoming out occurs and the maximum load surpasses the limit-load, substantially increasing the likelihood of injury in the lumbar region.

Fig. 5 demonstrates the increase in load as mass increases with varying attachment types. The maximum load measured is 36.64 kN, when the occupant is wearing the maximum equipment

Table 3
Effect of equipment mass and attachment type on minimum impact velocity needed to cause bottoming out.

Minimum impact velocity to cause bottom-out (m/s)				
Attachment type	Low [10,10,0.5]	Medium [20,20,1]	High [30,30,1.5]	Maximum [40,40,2]
Loose	9.6	9	8.5	8.2
Semi-tight	9.7	8.7	8.1	7.5
Tight	9.5	8.7	7.8	7.4

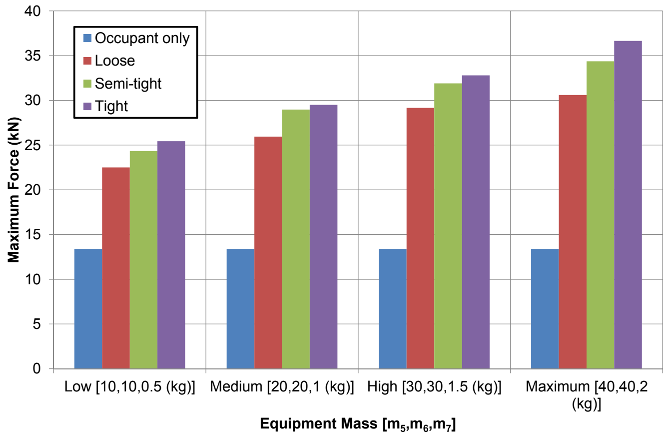

Fig. 5. Maximum seat force (force 1) with different equipment masses under different attachment conditions.

mass tightly attached. To investigate the effects of individual equipment locations, equipment masses were isolated. An equipment combination with 40 kg located at the hip and upper torso tightly attached produces a load of 35.71 kN, which is only 2.6% less than the maximum load, demonstrating that the head equipment mass has minimal effect on the load due to the distance between the head and the pelvis. This is supported by the case when only the head equipment is modelled; the maximum load is the limit load and does not cause seat bottoming out. Thus, the head equipment mass is considered to only have a substantial effect on the force on the head and neck injury.

3.4. Force on top of hip

The force on top of the hip is represented by force 2 in Fig. 1. Force 2 is a combination of the force from the viscera and the upper torso and contact force from the equipment and is measured to calculate the load on top of the hip. The force is calculated by

$$F_2 = c_{14}(\dot{x}_4 - \dot{x}_1) + k(x_4 - x_1) + c_{12}(\dot{x}_2 - \dot{x}_1) + k(x_2 - x_1) + c_{15}(\dot{x}_5 - \dot{x}_1) + k_{15}(x_5 - x_1) \tag{7}$$

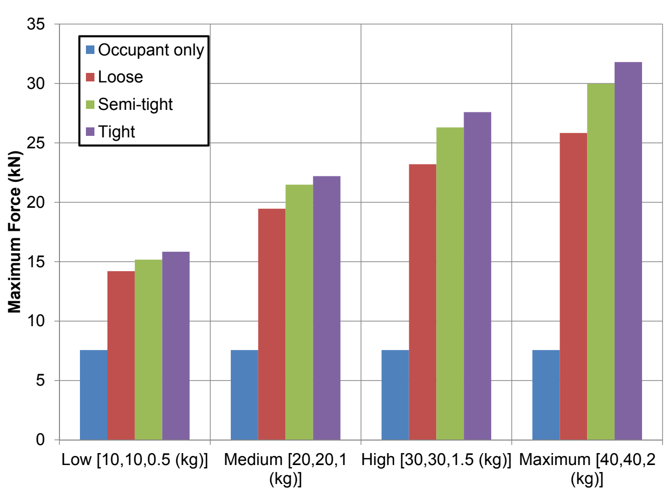

Fig. 6. Maximum force on the hip (force 2) with different equipment masses under different attachment conditions.

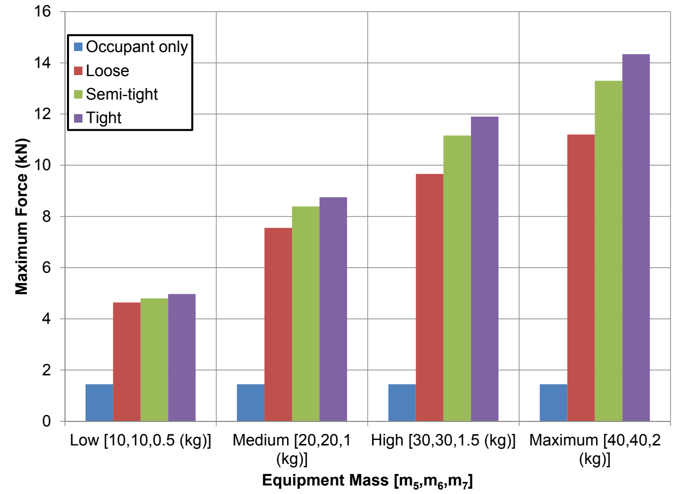

Fig. 7. Maximum force on the upper torso (force 3) with different equipment masses under different attachment conditions.

Fig. 6 illustrates the force on the hip with increasing equipment mass with different attachment types. As the equipment mass increases and the attachment type becomes tighter, the force increases. The greatest force on the hip is 31.81 kN, 321% greater than the occupant only. The head equipment mass has a minor effect on the force on the hip. When only the head equipment is modelled, the maximum force on the hip is 8.1 kN, 7.4% greater than the occupant without equipment. Furthermore, an equipment combination with 40 kg located at the hip and upper torso tightly attached produces a load of 31.28 kN, 1.68% less then when the maximum equipment mass is placed at all locations tightly. At each increment of equipment mass, the tight attachment produces the greatest force on the hip.

3.5. Force on the upper torso

The force on top of the upper torso is represented by force 3 in Fig. 1. The force is calculated by

$$F_3 = c_{23}(\dot{x}_3 - \dot{x}_2) + k_{23}(x_3 - x_2) + c_{26}(\dot{x}_6 - \dot{x}_2) + k_{26}(x_6 - x_2) \tag{8}$$

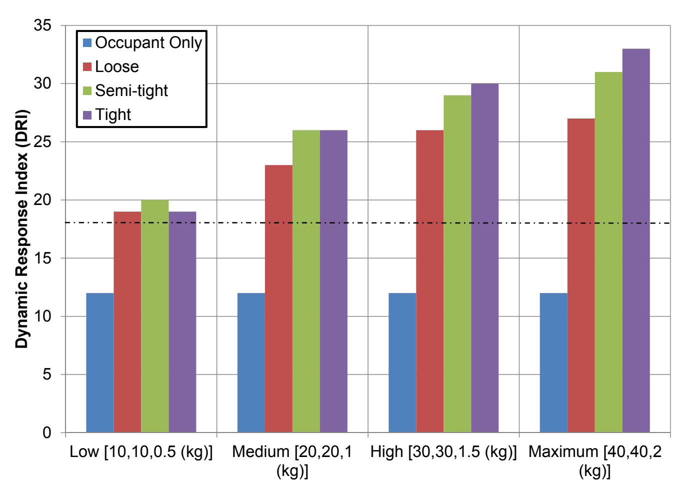

Fig. 8. Dynamic response index with different equipment masses under different attachment conditions.

Fig. 7 illustrates the force on the upper torso with increasing equipment mass with different attachment types. When the occupant is wearing all the equipment, the maximum force on the upper torso is 14.34 kN. Fig. 7 displays the maximum force measured at different equipment masses and attachment conditions. An equipment combination of 40 kg located at the hip and upper torso tightly attached produces a force on the upper torso of 13.94 kN, 2.87% less than the maximum force on the upper torso. Consequently, it is found that the head equipment mass has a minor effect on the force on the upper torso.

The dynamic response index (DRI) measures the likelihood of spinal injury in seat ejections; however, it can also be applied to impact cases. A DRI above 18 correlates with a 10% chance of spinal injury and is the threshold for crashworthy seats. The DRI is calculated by

$$\mathrm{DRI} = \frac{\omega_n^2}{g}X \tag{9}$$

where ω_n is 52.9 based on experimental tests of U.S. Military Airforce (Payne and Stech, 1969), g is acceleration due to gravity and X is the maximum displacement between m_2 and m_1.

Fig. 8 illustrates the DRI with increasing equipment mass with different attachment types. Without equipment, the model registers a DRI of 12 corresponding to less than 0.2% probability of spinal injury. When the maximum equipment mass is tightly attached at all locations, a DRI of 33 is measured, which correlates to more than 50% chance of spinal injury. When the equipment is isolated, the upper torso equipment mass has the greatest effect on the DRI. When the occupant is only wearing 40 kg tightly attached at the upper torso, a DRI of 32 is measured, indicating the minimal effect of the hip and head equipment masses on the DRI.

3.6. Force on the head

The force on top of the head is represented by force 4 in Fig. 1. The force is calculated by

$$F_4 = c_{37}(\dot{x}_7 - \dot{x}_3) + k_{37}(x_7 - x_3) \tag{10}$$

Fig. 9 demonstrates with the increase in equipment mass, the force on the head from the head equipment mass increases. The maximum force on top of the head when all the equipment is modelled is 0.709 kN, however, with only head equipment, the maximum force is 0.770 kN which is 8.6% greater than when all the equipment is modelled. As this force is a contact force from the head equipment mass, the head equipment mass has the most substantial effect. When the occupant is wearing upper torso mass the accelerations of the head decrease causing m_2 to become more rigid. Consequently, when only the head equipment is modelled, the force on the head is greater. The combination of the hip and head equipment causes a 36% increase in force on the head than the combination of upper torso and head equipment supporting the theory that the upper torso equipment mass reduces the head accelerations.

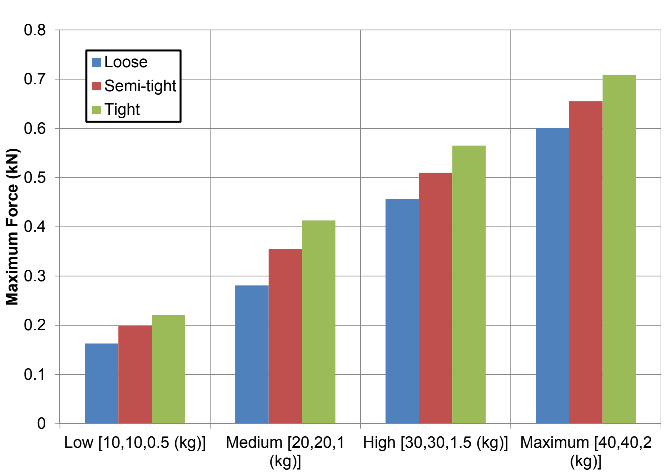

Fig. 9. Maximum force on the head (force 4) with different equipment masses under different attachment conditions.

4. Discussion and limitations

4.1. Effect of increasing equipment mass

The results illustrate that increasing equipment mass will increase the forces experienced by the occupant at all locations and will cause seat bottoming out much earlier with a heavier equipment mass. In a study by Richards and Sieveka (2011), it was determined that the occupant would experience a greater lumbar load depending on seating configuration when the individual was wearing 20 kg of upper torso equipment mass. In the present study, it was determined that, with equipment placed at the lower torso, upper torso and head, it will substantially increase the chances of an occupant experiencing injurious forces at the lower torso, upper torso and head.

Once seat bottoming out occurs, the forces experienced by the occupant are substantially increased past the stroking load limit. The increase in weight increases the chances of seat bottoming out and therefore the energy absorption device is no longer able to protect the occupant at loads under the humanly tolerable limit. A report completed by the Transportation Safety Board of Canada (2009) found that all seats, which bottomed-out, subjected the occupants to loads exceeding the loads experienced by the occupants, who were seated in seats that prevented bottoming out from occurring. In Fig. 4 the occupant without equipment is protected from excessive loads until seat bottoming out occurs. Once this happens, the seat no longer acts as a crashworthy seat, but subjects the occupant to extremely high loads, which pass the limit load.

A solution to prevent seat bottoming out would be to provide ample space between the seat pan and the cabin floor to allow the seat to stroke until it absorbs the entire impact energy. However, there are constraints with cabin space. Another solution, is to remove all equipment from the occupants, or utilise a quick strip mechanism, that when the individual is aware they are going to crash, this switch, removes all the equipment from their body. As seen in Fig. 2(b), the equipment is generally held in what is called a primary survival gear carrier and therefore utilising a switch that eliminates the equipment from the body, will allow the occupant not to experience the loads generated during seat bottoming out.

Seat certification tests for occupants require the seat be designed to absorb the impact energy with an occupant that weighs 91 kg with 5 kg of equipment (Military Standard-58095A, 1986). Currently military equipment exceeds 30 kg and therefore a 50th percentile male occupant weighing 77 kg with 30 kg of equipment exceeds the standard certification requirements. Current certification tests should be expanded to accommodate current military equipment lists. Furthermore, utilising a variable load energy absorption (VLEA) seat rather than an FLEA seat would improve the chances of impact energy being absorbed prior to the end of stroke. A VLEA seat allows the occupant to turn the knob to calibrate the energy absorption limit load to cater for the user's weight. Seat certification tests require the seat to be able to fully absorb the entire impact energy and protect the occupant under the designated limit load over a maximum change in velocity. The present study, found the seats ability to absorb the impact energy within the stroking length at higher initial impact velocities reduces with increasing equipment mass and therefore the safe velocity the seat is certified too is no longer valid with an increased equipment mass.

4.2. Effect of attachment type

The analysis demonstrates that loose attachment would be most beneficial to reduce the force on the occupant; however, it is unrealistic to have all the equipment loosely attached as the equipment would move all about the cabin. Loosely attached equipment may increase the chances of contact injury and create loads in different loading paths. Furthermore loose equipment would also create a greater likelihood of snagging during an egress of the helicopter after impact.

The tight equipment attachment provides the greatest force because the high stiffness coefficient causes the loading path of the equipment to be the same as the loading path of the occupant. In real world operations, it is assumed that the tighter the equipment is attached to the occupant, the greater chance the load will follow the loading path and in phase with the occupant. Consequently, if the same simulation were to be conducted in three dimensions, the loose equipment attachment would demonstrate higher loads in the loading paths in the x and y directions as well as z.

4.3. Limitations

The model used in this study has obvious limitations in its ability to analyse the occupant with body-borne equipment in 3 dimensions. Furthermore distributing the equipment over the upper torso as demonstrated in Fig. 2 is difficult to model in one dimension. A more complex model with 3 dimensions would be able to determine the effects of equipment off-loading paths and its subsequent effect on the forces on the occupant and its influence on the seats ability to absorb the entire impact energy during stroke, before seat bottoming-out occurs.

5. Conclusion

A seven-DOF lumped parameter model was utilized to study the effects of a seated occupant wearing body-borne equipment on a crashworthy seat during a simulated helicopter crash. The three stages of an FLEA mechanism used in a crashworthy seat during a helicopter crash were simulated in the biomechanics model. The study was conducted to determine the effect of equipment mass on the forces experienced by an occupant during a simulated helicopter crash. From the analysis and validation the following conclusions can be drawn.

1. Dimensional analysis shows that the maximum forces on the occupant are proportional to the initial impact velocity before stroke occurs.
2. Tight attachment generated the greatest force at all locations. This is due to the loading path following the one-dimensional vertical loading path used in this analysis. As such, it would be worthwhile to attach everything loosely, however, in real operations, the chance of contact injury and different loading paths due to the equipment flailing everywhere would increase.
3. As equipment mass increases, the minimum initial impact velocity needed to cause seat bottoming out decreases. When the model has equipment attached, the seat is unable to absorb the total impact energy and prevent bottoming out at a lower initial impact velocity. However, when the model is without equipment, the seat is able to withstand a higher initial impact velocity, but as equipment mass is added and increased the seats ability to absorb the impact energy at higher initial impact velocities reduces.
4. Equipment mass increases the loading on the occupant at all locations measured.

These conclusions demonstrate the effect of increased equipment mass on an occupant and the effect of attachment type on the loading of the equipment. A simplified solution in the real world to the problems associated with equipment mass increasing the forces on the occupant and potential injury is to remove all military gear on the occupant. However, from an operational standpoint, this is not practical, as military personnel are required to wear certain items to protect them in tactical and combat missions. Further studies, could be completed to investigate equipment off-loading paths by using a 3 dimensional model. Furthermore determining the effects of mass-distribution on these forces will help to develop a better method to place the equipment over the body. Yet, for the purpose of this study, the model was able to effectively investigate the forces experienced by an occupant in the vertical direction, and the effects of equipment attachment type.

Conflict of interest

The authors have no conflict of interest.

References

Boileau, P.E., Rakheja, S., 1998. Whole-body vertical biodynamic response characteristics of the seated vehicle driver: measurement and model development. Int. J. Ind. Ergonom. 22, 449–472.
Buckingham, E., 1914. On physically similar systems; illustrations of the use of dimensional equations. Phys. Rev. 4, 345–376.
Coltman, J.W., 1994. Rotorcraft Crashworthy Airframe and Fuel System Technology Development Program (Report DOT/FAA/CT-19/7). Federal Aviation Administration, Washington DC.
Desjardins, S.P., 2003. The evolution of energy absorption systems for crashworthy helicopter seats. In: The Proceedings of the American Helicopter Society 59th Annual Forum, Phoenix, Arizona.
Dong, Y.P., Lu, Z.H., 2012. Analysis and evaluation of an anti-shock seat with a multistage non-linear suspension for a tactical vehicle under a blast load. J. Autom. Eng. 226 (8), 1037–1047.
Forde, K.A., Albert, W.J., Harrison, M.F., Neary, J.P., Croll, J., Callaghan, J.P., 2011. Neck loads and posture exposure of helicopter pilots during simulated day and night flights. Int. J. Ind. Ergonom. 41, 128–135.
Liang, C.C., Chiang, C.F., 2006. A study on biodynamic models of seated human subjects exposed to vertical vibration. Int. J. Ind. Ergonom. 36, 869–890.
Mathys, R., Ferguson, S.J., 2012. Simulation of the effects of different pilot helmets on neck loading during air combat. J. Biomech. 45, 2362–2367.
Military Specification MIL-S-58095A, 1986. Seat System: Crash Resistant, Nonejection, Aircrew General Specification for. Department of Defense, Washington D.C.
Mills, N., 2007. Seating case study. In: Polymer Foams Handbook – Engineering and Biomechanics Applications and Design Guide. Elsevier Jordan Hill, Oxford, p. 224.
Naval Air Systems Command, NAVAIR 13-1-6.7.2, May 1999. Aircrew Personal Protective Equipment, Washington D.C. (accessed 01.04.07).
Payne, P.R., Band, E.G., 1971. A Four-degree-of-freedom Lumped Parameter Model of the Seated Human Body. Aerospace Medical Research Laboratory.
Payne, P.R., Stech, E.L., 1969. Dynamic Models of the Human Body. Aerospace Medical Research laboratory.
Richards, M., Sieveka, E., 2011. The effects of body-borne equipment weight on ATD lumbar loads measured during crashworthy seat vertical dynamic tests. In: Proceedings of the American Helicopter Society 67th Annual Forum, Virginia Beach, Virginia.
Rao, S.S., 2005. Equivalent masses, springs and dampers. In: Mechanical Vibrations. SI Edition, Singapore.
Transportation Safety Board of Canada, 2009. Main Gearbox Malfunction/Collision with Water (Report number A09A0016). Cougar helicopters Inc.
Wan, Y., Schimmels, J.M., 1995. A simple model that captures the essential dynamics of a seated human exposed to whole body vibration. Adv. Bioeng., ASME, BED 31, 333–334.
Wang, J., Bird, R., 2000. Improved seating to protect occupants of vehicles from landmines. In: Proceedings of the Land Warfare Conference. Melbourne, Victoria.
Yan, W., Kan, Q., Kergrene, K., Kang, G., Feng, X.-Q., Rajan, R., 2013. A truncated conical beam model for analysis of the vibration of rat whiskers. J. Biomech. 46, 1987–1995.
Zong, Z., Lam, K.Y., 2002. Biodynamic response of shipboard sitting subject to ship shock motion. J. Biomech. 35, 35–43.